

Empirical Terrain Models for Surface Wind and Air Temperature over Iceland

Nikolai Nawri
Halldór Björnsson
Guðrún Nína Petersen
Kristján Jónasson

Empirical Terrain Models for Surface Wind and Air Temperature over Iceland

Nikolai Nawri, Icelandic Met Office
Halldór Björnsson, Icelandic Met Office
Guðrún Nína Petersen, Icelandic Met Office
Kristján Jónasson, University of Iceland

Keypage



Report no.: VÍ 2012-009	Date: September 2012	ISSN: 1670-8261	Public <input checked="" type="checkbox"/> Restricted <input type="checkbox"/> Provision:
Report title / including subtitle Empirical Terrain Models for Surface Wind and Air Temperature over Iceland		No. of copies: 20 Pages: 33	
Authors: Nicolai Nawri Halldór Björnsson Guðrún Nína Petersen Kristján Jónasson		Managing director: Jórunn Harðardóttir	
		Project manager: Halldór Björnsson	
Project phase:		Project number: 5813-0-0004	
		Case number: 2012-333	
Report contracted for: IceWind Project			
Prepared in cooperation with:			
Summary: In this study, gridded empirical terrain models for surface wind speed and air temperature over Iceland are developed based on station data, whereby average fields are determined for individual months, and for different intensities of large-scale pressure gradients. In winter, prevailing downslope and offshore surface wind occurs across Iceland, with negligible differences between day and night. In summer, significant differences exist, both in speed and direction, between day- and night-time surface wind conditions. Under weak and intermediate large-scale pressure gradients, the monthly correlation between the geostrophic wind speed and measured surface wind speed at individual locations is generally poor. At some locations, correlation between surface and geostrophic wind speed improves with increasing strength of the overlying circulation, especially in winter.			
Keywords: Surface wind speed and direction, surface air temperature, effects of large-scale circulation, station data, gridded surface measurements, Iceland		Managing director's signature: 	
		Project manager's signature:	
		Reviewed by:	

Contents

1	Introduction	7
2	Data	8
3	Orographic Effects	9
4	Accuracy of Terrain Models	15
5	Reference Values at Mean Sea Level	18
6	Gridded Fields	22
7	Effects of the Large-Scale Atmospheric Circulation	25
8	Summary	31

List of Figures

1	Terrain elevation of the WRF model	9
2	Terrain elevation and distance to the coast or to the open ocean	10
3	Mean monthly surface wind speed as a function of terrain elevation	11
4	Correlation of surface wind speed and temperature with local terrain elevation	12
5	Mean monthly surface air temperature as a function of terrain elevation	13
6	Errors associated with the one-parameter terrain models	17
7	Monthly vertical gradients of wind speed and air temperature	19
8	Monthly surface wind speeds at station locations	20
9	Monthly surface air temperatures at station locations	21
10	Gridded wind speed based on the one-parameter terrain model	23
11	Gridded horizontal wind vectors at mean sea level	24
12	Gridded air temperature based on the one-parameter terrain model	25
13	Correlation between surface air speed and geostrophic wind speed	27
14	Correlation between surface and geostrophic wind speed for smoothed time-series	28
15	Terrain gradients of surface wind speed for different geostrophic wind speeds	29
16	Gridded surface wind speed for different geostrophic wind speeds	30

1 Introduction

In this study, gridded empirical terrain models for surface wind speed and air temperature over Iceland are developed based on station data, whereby average fields are determined for individual months, and for different intensities of large-scale pressure gradients. Large areas of the island are sparsely covered by the operational network of weather stations, with some neighbouring stations separated by tens of kilometres. Although differences in monthly averages between these locations usually suggest moderate gradients, as shown in a related study (Nawri et al., 2012c), large differences in monthly averages, particularly in wind speed, are found among several nearby stations, which are primarily due to differences in terrain elevation. Due to the complex interjacent orography, existing data are not sufficient to linearly interpolate between stations, without taking into account at least the variability of terrain elevation at and between measurement sites.

The simplest approach to parameterising the spatial variability of average atmospheric fields is to assume a linear dependence on height above mean sea level, that is uniform across the domain. This vertical gradient is determined through least squares regression analysis. By subtracting the linear model from the actual measurements, residual values at mean sea level are obtained, which are then horizontally interpolated onto a regular grid. Interpolated values on the elevated terrain are obtained by adding again the linear model to the gridded field at mean sea level.

This methodology is similar to that employed in previous studies for monthly surface air temperature over Iceland, although differences exist in parameterisation and horizontal interpolation, as described in detail below. Björnsson et al. (2007) developed an eight-parameter terrain model, using longitude, latitude, terrain elevation, distance to the open ocean, and the first four eigenvectors of the local topography. Horizontal interpolation onto a 1-km grid was done through kriging. This model is based on a simpler version developed by Gylfadóttir (2003), which does not use the eigenvectors of terrain elevation. Crochet and Jóhannesson (2011) developed a one-parameter terrain model with a constant vertical lapse rate of 6.5 K km^{-1} . Horizontal interpolation onto a 1-km grid was done using tension-splines.

As outlined in the introduction to Nawri et al. (2012c), the study presented here is also part of research conducted in the context of the project “Improved Forecast of Wind, Waves and Icing” (IceWind), Work Package 2, with the ultimate goal of developing a wind atlas for Iceland, primarily for the assessment of wind energy potential. Central to this project are mesoscale model runs, produced by Reiknistofu í veðurfræði in the context of “Reikningar á veðri” (RÁV) (Rögnvaldsson et al., 2007, 2011), with a special setup of the Weather Research and Forecasting (WRF) Model (Skamarock et al., 2008). In a follow-up study (Nawri et al., 2012a), local station data and the gridded terrain models for surface wind, developed here, will be compared with WRF model simulations. The statistical correction of WRF model data based on these comparisons is discussed in Nawri et al. (2012b).

2 Data

Quality controlled hourly surface measurements of wind speed and direction, as well as air temperature, were obtained from the Icelandic Meteorological Office (IMO). Winds are measured at different heights, h , above ground level (AGL), varying between 4.0 and 18.3 m. These differences are taken into account following WMO guidelines (WMO, 2008), whereby wind speeds are projected to 10 mAGL by

$$S(10\text{m}) = S(h) \frac{\ln(10/z_0)}{\ln(h/z_0)}, \quad (1)$$

where for Iceland the surface roughness length z_0 over land is approximately 3 cm (Troen and Petersen, 1989). Surface air temperature is measured at 2 mAGL. As described in Nawri et al. (2012c), for any given variable, only those locations are considered, for which station records have at least 75% valid data within any specific period under consideration. The names, ID numbers, and coordinates of all stations from which data was used are given in Nawri et al. (2012c) (see the appendix there). For comparison with the related studies mentioned in the introduction (Nawri et al., 2012c,a,b), the hourly observational time-series were reduced to 3-hourly values, to be consistent with the WRF model data. This study also covers the same 4-year period from 1 Nov 2005 until 31 Oct 2009.

As discussed in Nawri et al. (2012c), at three stations with a good data recovery rate (i.e., Station 1496 (Skarðsmýrarfjall), Station 6017 (Stórhöfði), and Station 5960 (Hallormsstaðaháls)), the measured wind speeds are clear outliers relative to nearby measurements, due to exposed or elevated anemometer positions. Since the wind statistics at these stations are not representative of locations only a few kilometres away, these time-series are excluded from the analysis.

An important part of the analysis is the calculation of the changes with terrain elevation of surface wind speed and air temperature. To be able to compare these vertical terrain gradients with vertical gradients in the boundary-layer atmosphere, operational radiosonde data from Keflavík airport were obtained from IMO. The upper-air station is located at 22.600°W and 63.950°N, at the tip of Reykjanes peninsula, at an elevation of 52.0 m. The vertical profiles are therefore representative of the coastal and maritime boundary-layer. Radiosondes are released twice-daily at 11:30 and 23:30 UTC. The data recovery rate is 3 seconds.

To determine the dependence of vertical terrain gradients, as well as the horizontal variability of wind speed, on the large-scale atmospheric circulation, 6-hourly operational analyses of geopotential height at 850 hPa were obtained from the European Centre for Medium-Range Weather Forecasts (ECMWF), for the calculation of the geostrophic wind at that level. Analysis fields are valid at 00, 06, 12, and 18 UTC (which is local time in Iceland throughout the year). The angular grid-spacing is 0.250 degrees in longitude, and 0.125 degrees in latitude, corresponding to a physical grid-spacing of 13.9 km in latitude, and 11.7 km in longitude, along 65°N. The 6-hourly fields are linearly interpolated onto the 3-hourly time-axis of the observational data.

For consistency with the related studies mentioned in the introduction, the horizontal RÁV WRF model grid is used here as a basis for the terrain models. It has a grid-point spacing of about 3 km. Also used from this model setup is the gridded terrain elevation (see Figure 1).

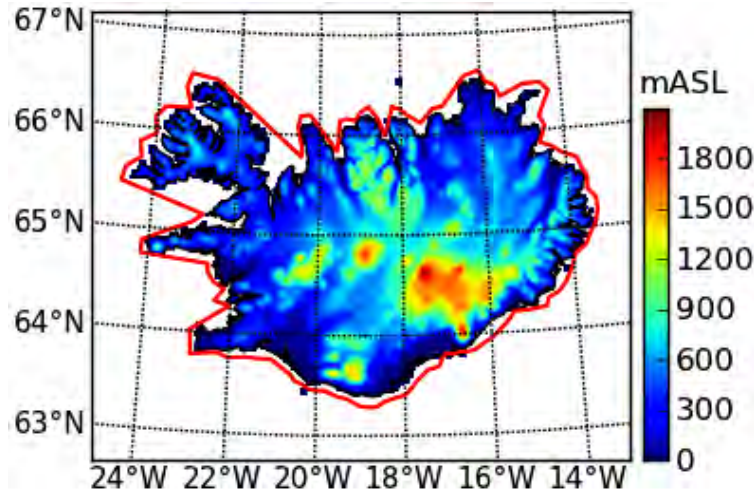


Figure 1. Terrain elevation of the WRF model, with 3-km grid-point spacing. The red line indicates the boundary between near coastal waters and the open ocean, as defined in Section 2.

For the calculation of the shortest horizontal distances¹ from station locations and model land grid-points to the coast, coastline data from the National Geophysical Data Center of the U. S. National Oceanic and Atmospheric Administration is used. Due to the presence of several long but narrow and sheltered fjords along the coast of Iceland, in addition to distance to the coast, also the shortest horizontal distances to the open ocean are calculated. For this, the boundary between open ocean and near coastal waters needs to be defined. This is done here by calculating the maximum distance of the coastline from a point near the centre of the island (18.35°W and 64.77°N), for each 3-degree sector originating from that point. The resulting line is then uniformly moved 10 km further away from the coast (see Figure 1).

3 Orographic Effects

In this study, single-parameter empirical terrain models for surface wind speed and air temperature are developed, individually for each month, and for different intensities of the geostrophic wind at 850 hPa. Among the main terrain-related parameters, which can be expected to have strong and systematic effects on surface wind speed and air temperature, are elevation and distance to the coast (DTC) or to the open ocean (DTO).

In the case of wind speed, elevation and DTC/DTO have opposing effects, with wind speed generally increasing with height, and decreasing away from the coast. Surface air temperature generally decreases with height, whereas the magnitude of the seasonal cycle increases away from the coast. Assuming homogeneity of ground surface type and overlying atmospheric conditions, spatial variability of surface wind speed and air temperature can then be expected to be the result of a combination of the effects of the two basic terrain-related parameters. In the case of Iceland,

¹All horizontal distances in this study are calculated along great circles on a spherical Earth at mean sea level.

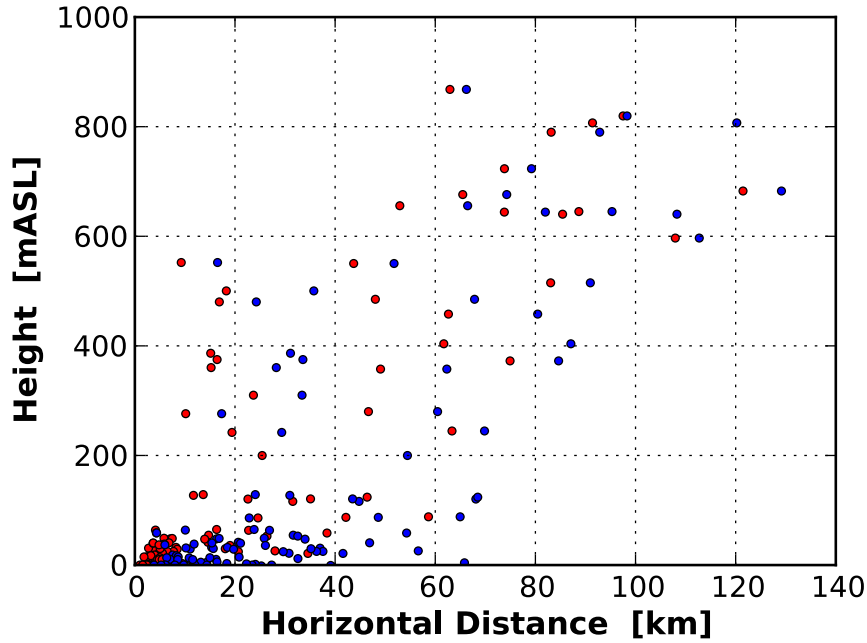


Figure 2. Relationship between terrain elevation and horizontal distance to the coast (red dots) or to the open ocean (blue dots) at station locations.

terrain elevation generally increases away from the coast (see Figure 1). As shown in Figure 2, this is specifically true at station locations. Therefore, the effects of terrain elevation and DTC/DTO cannot be separated properly, based on the available station data.

Linear correlations between terrain elevation and surface wind speed at all station locations (0.46 in January and July) are higher than the correlations between DTC and surface wind speed (0.30 in January, 0.35 in July), or the correlations between DTO and surface wind speed (0.22 in January, 0.33 in July). Moreover, the sign of the DTC/DTO correlations is opposite to what would be expected. Correlations between terrain elevation and surface air temperature (-0.91 in January, -0.69 in July) are also higher than the correlations between DTC and surface air temperature (-0.78 in January, -0.38 in July), or the correlations between DTO and surface air temperature (-0.80 in January, -0.35 in July). Therefore, given the geography of Iceland, for surface wind speed and air temperature, elevation is the most dominant geographical parameter, and will be used here for the development of simple terrain models.

Mean monthly terrain-following profiles of surface wind speed, together with vertical atmospheric profiles derived from radiosonde data, are shown in Figure 3. In this and all following figures, height is always referring to measurement height (terrain elevation plus sensor height). Up to distances of 6 km from the coast, stations are located exclusively below 100 mASL, and yet show a significant spread in average monthly values. This is due to the fact that some coastal stations are located either within sheltered fjords, or on exposed headlands and peninsulas. The correlation of mean monthly wind speeds with height, as a function of the minimum distance to the coast, is shown in Figure 4. As stations at increasing distances from the coast are being excluded from the calculation, correlation increases rapidly up to a minimum distance of 6 km, remaining essentially constant for cut-off distances further inland. If coastal stations were included, the large variability

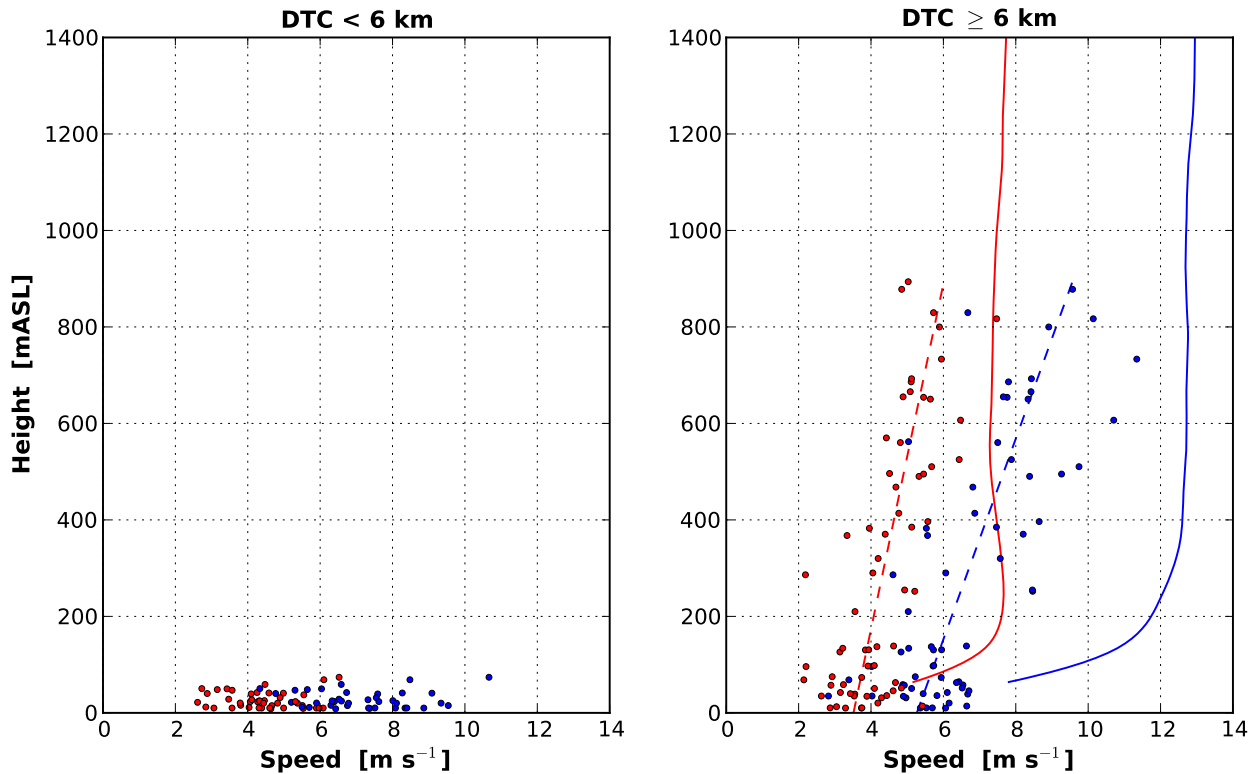


Figure 3. Mean monthly surface wind speeds at station locations in January (blue dots) and July (red dots) as a function of terrain elevation. Stations are separated by distance to coast (DTC). The dashed lines represent best linear fits to the monthly data points. The solid lines are mean monthly radiosonde profiles from Keflavík Airport.

at low elevations near the coast would unduly influence the parameterisation of the more systematic dependence of surface wind conditions on terrain elevation in the interior. To be representative for the main part of the island, stations at distances from the coast of less than 6 km are therefore excluded from the calculation of vertical terrain gradients of surface wind speed. Nonetheless, the model is extended to the coast by the inclusion of all stations, whereby the projection to mean sea level based on the inland stations is applied uniformly. Referring back to Figure 3, despite increasing terrain elevation towards the interior, due to the counter-acting effects of increased surface roughness for winds from the coast, surface wind speeds increase considerably slower than wind speeds in the boundary-layer atmosphere at the same height above mean sea level. As a result, at distances of at least 6 km from the coast, the dependence of surface wind speed on terrain elevation is best represented by a linear profile, derived by least-squares fit, rather than the logarithmic one, which exists in the boundary-layer atmosphere. Projecting the linear profiles to above the highest station elevation, surface wind speeds approach the free atmospheric values at about 1500 mASL in winter, and at 1400 mASL in summer.

The equivalent results for surface air temperature are shown in Figure 5. Similar to surface wind speed, although to a lesser extent, there is some spread in monthly averages at low-lying locations near the coast, particularly in summer. As shown in Figure 4, correlation between temperature and the negative of elevation is consistently high, even if near coastal stations are included. However,

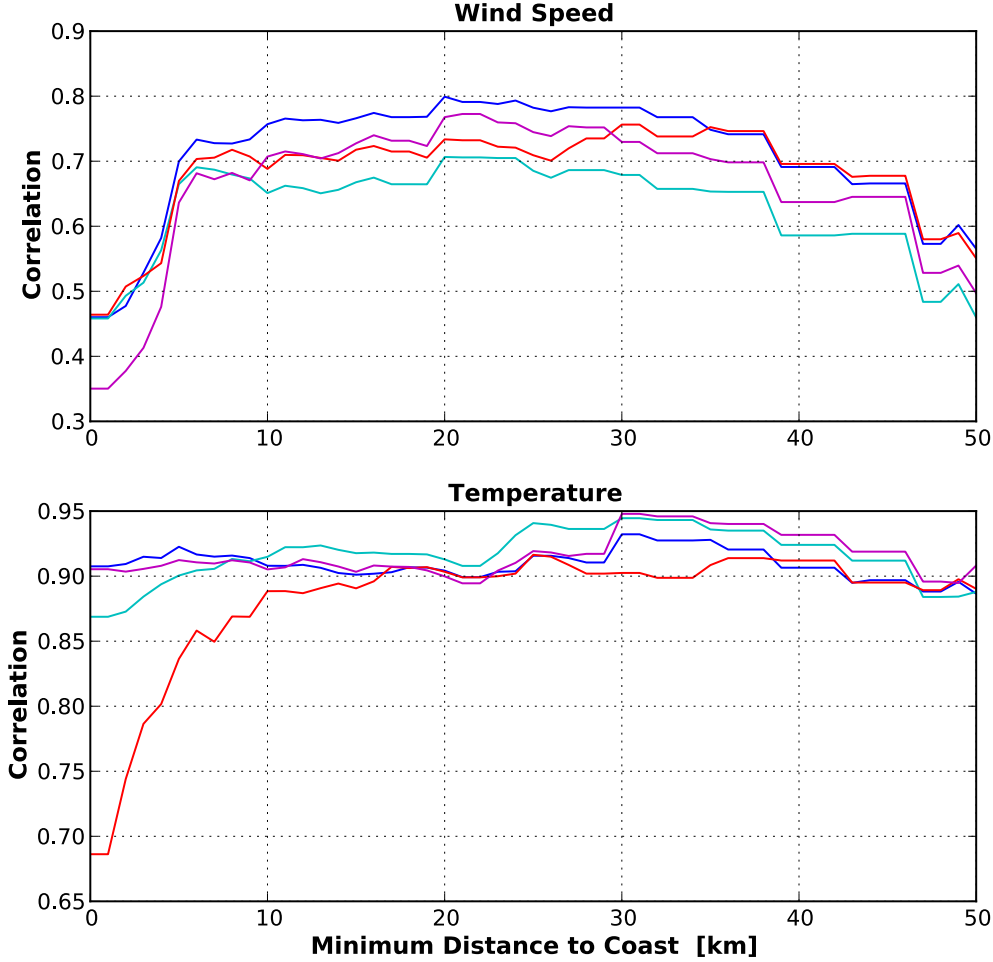


Figure 4. Correlation of monthly mean surface wind speed with local terrain elevation, and correlation of monthly mean surface air temperature with the negative of local terrain elevation as functions of the minimum distance to coast for which station data is included, for January (blue lines), April (cyan lines), July (red lines), and October (magenta lines).

in summer, correlation increases, if locations less than 6 km from the coast are excluded. As for surface wind speed, the calculation of vertical terrain gradients is therefore limited to stations at least 6 km from the coast. Referring back to Figure 5, in summer, the differences between surface air temperatures and boundary-layer temperatures at the same height above mean sea level are negligible. However, in winter, despite identical lapse rates, temperatures over the elevated terrain in the interior of the island are about 3°C lower than in the coastal and maritime boundary-layer, which is represented by the radiosonde profiles. This is to be expected based on the increased longwave radiation losses over land in winter, especially in the presence of snow.

In the one-parameter terrain models, the dependence on height of surface measurements is determined by linear vertical terrain gradients, i.e., by changes with height above mean sea level along the surface of elevated terrain. The height above mean sea level of surface measurements at the i -th station location, $\mathbf{x}_i = (x_i, y_i)$, is given by $z_i = z(\mathbf{x}_i) + h_0$, with local terrain elevation $z(\mathbf{x}_i)$, and sensor height above ground h_0 (= 10 mAGL for surface wind speed, and 2 mAGL for surface air temperature).

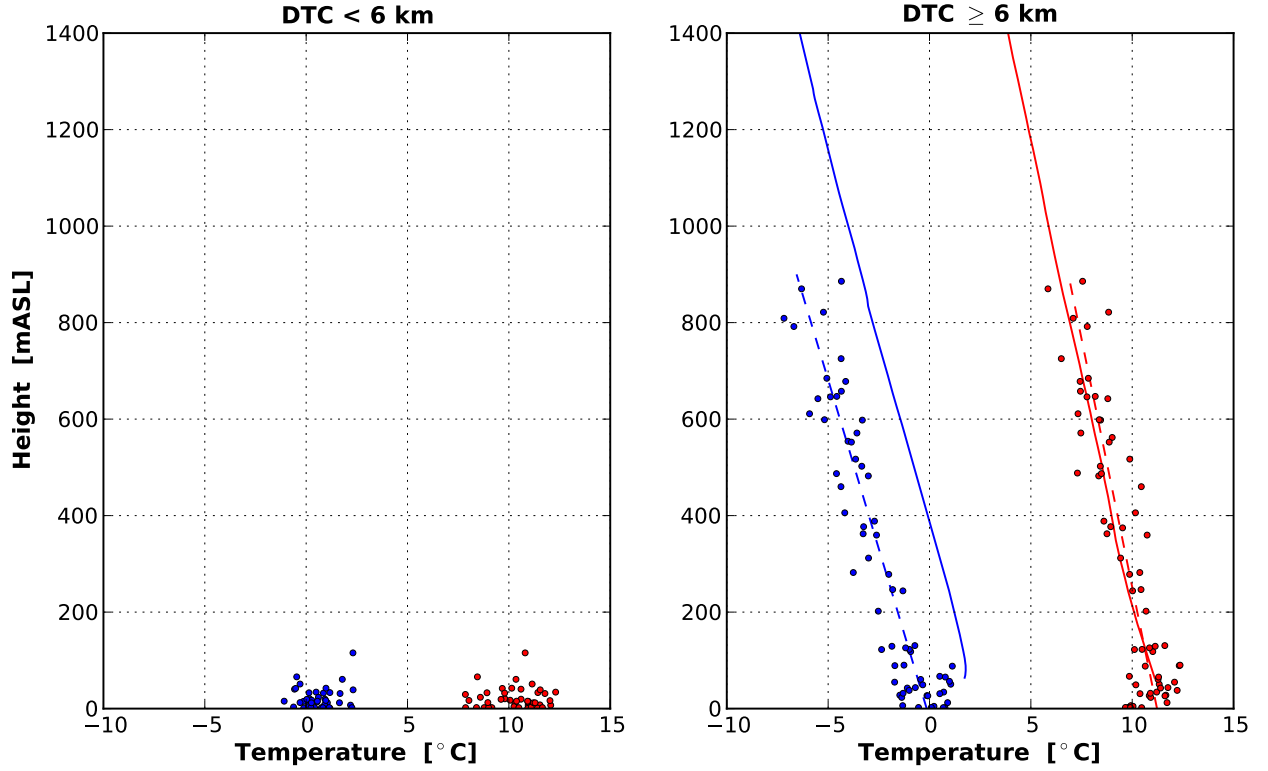


Figure 5. Mean monthly surface air temperatures at station locations in January (blue dots) and July (red dots) as a function of terrain elevation. Stations are separated by distance to coast (DTC). The dashed lines represent best linear fits to the monthly data points. The solid lines are mean monthly radiosonde profiles from Keflavík Airport.

For each month, and for different intensities of the geostrophic wind speed, the local averages of surface variables, s_i , at station heights, z_i , are calculated. Based on these, a linear least squares approximation of the vertical dependence of the respective variable is given by

$$s(z) = cz + d, \quad (2)$$

with constants c and d determined by linear regression. As seen in the following sections, these simple models capture much of the spatial dependence of surface wind speed and air temperature. However, there is spread around the linear profile, which is the result of horizontal differences at the same height. Regional differences which are not due to terrain elevation are therefore taken into account by allowing horizontal dependence of the mean sea level ($z = 0$) value, d , such that

$$s(x, y, z) = cz + d(x, y) \quad (3)$$

with the same vertical gradient, c , from the linear least squares fit. The gridded horizontal reference field, $d(x, y)$, at mean sea level is derived from the local values

$$d(x_i, y_i) = s(x_i, y_i, z_i) - cz_i \quad (4)$$

by horizontal interpolation.

Several methods for horizontal interpolation are compared here: 1) linear radial basis functions, preserving local values; and 2) various types of horizontal averaging, not preserving local values, and resulting in smoothing of gradients. The relative accuracy of the two methods depends on how well local values represent the typical values within about half the distance towards neighbouring stations. Although preferable with regionally representative measurements, interpolation techniques preserving local values give too much weight to those places, where measurements are heavily influenced by local factors.

Based on radial basis functions, the interpolated value at any location $\mathbf{x} = (x, y)$ is given by

$$f(\mathbf{x}, t) = \sum_j w_j(t) \phi(|\mathbf{x} - \mathbf{x}_j|) , \quad (5)$$

where the weights w_j of the chosen radial basis functions $\phi(|\mathbf{x} - \mathbf{x}_j|)$ are determined by solving the linear system of algebraic equations, derived from the requirement, that the interpolated field be identical to the values at all station locations,

$$\sum_j w_j(t) \phi(|\mathbf{x}_i - \mathbf{x}_j|) = f(\mathbf{x}_i, t) . \quad (6)$$

By inverting the symmetrical matrix $\Phi_{ij} = (|\mathbf{x}_i - \mathbf{x}_j|)$, the solution in matrix notation is given by $w_i = \Phi_{ij}^{-1} f_j$, with $f_j = f(\mathbf{x}_j, t)$. Since there is no physical justification for using any particular nonlinear interpolation function for averages at mean sea level, the simplest case of linear radial basis functions,

$$\phi(|\mathbf{x} - \mathbf{x}_i|) = |\mathbf{x} - \mathbf{x}_i| , \quad (7)$$

is used here.

Interpolation onto the regular grid at mean sea level through horizontal averaging uses horizontally variable weighting functions $r(\mathbf{x}, \mathbf{x}_i)$. With the original field, f , specified at station locations, \mathbf{x}_i , the value at grid-point \mathbf{x} of the interpolated field, g , derived from f by regional averaging, is given by

$$g(\mathbf{x}) = \frac{\sum_i r(\mathbf{x}, \mathbf{x}_i) f(\mathbf{x}_i)}{\sum_i r(\mathbf{x}, \mathbf{x}_i)} . \quad (8)$$

The weighting functions tested here can generally be written as

$$r(\mathbf{x}, \mathbf{x}_i) = \exp(-a_0 |\mathbf{x} - \mathbf{x}_i| - c_0 |D(\mathbf{x}) - D(\mathbf{x}_i)|) , \quad (9)$$

where $D(\mathbf{x})$ is the shortest horizontal distance to the coast or to the open ocean, and coefficients a_0 and c_0 are positive. The weighting decreases with horizontal distance of a given grid-point from any of the station locations, as well as with the absolute difference in DTC/DTO. It is therefore a combined measure of spatial proximity and geographical similarity with respect to the distance from the coast, or the open ocean.

Gridded monthly reference fields of the horizontal wind components at mean sea level are defined as

$$u(x, y) = -d(x, y) e_x(x, y) \quad (10)$$

$$v(x, y) = -d(x, y) e_y(x, y) , \quad (11)$$

where $\mathbf{e}(x, y) = (e_x(x, y), e_y(x, y))$ is the corresponding monthly average of the gridded field of horizontal unit vectors pointing into the direction of the wind vector. Gridded fields of unit vectors are calculated from the local values $(-\sin \phi(x_i, y_i), -\cos \phi(x_i, y_i))$ through horizontal averaging, where wind direction ϕ in radians is defined, as usual, as the direction from which the wind is blowing. The weighting function used for the interpolation of unit vectors only depends on the distance from any of the station locations,

$$r(\mathbf{x}, \mathbf{x}_i) = \exp(-a_0 |\mathbf{x} - \mathbf{x}_i|) . \quad (12)$$

Since at low wind speeds wind direction is ill defined, when calculating average unit vectors, wind speeds of less than 1 m s^{-1} are excluded.

4 Accuracy of Terrain Models

An estimate of the errors associated with the empirical terrain models can be obtained by excluding individual stations from the analysis outlined in the previous section, and comparing the interpolated values from the terrain model with the excluded station data. This procedure is discussed in more detail in Gylfadóttir (2003) and Björnsson et al. (2007). The errors from cross-predictions for surface wind speed and air temperature within each month were calculated for each of the horizontal interpolation techniques discussed in the previous section.

For horizontal averaging, special cases of the weighting function were tested:

1) Constant weighting function ($a_0 = c_0 = 0$), resulting in reference fields with a constant value equal to the arithmetic mean of all values projected to mean sea level.

2) Weighting function depending only on horizontal distance, with $c_0 = 0$ and $a_0 = \log(2)/h_a$. The choice of the half-width h_a determines the spatial variability of the resulting interpolated field. In the limit of increasing the half-width to infinity, the weighting function becomes constant and equal to one, resulting in an arithmetic mean of all values $f(\mathbf{x}_i)$ at each grid-point. In regions with a high density of stations, distant values may then have too much influence. Conversely, for very short half-widths, the weighting coefficients become negligibly small, except for those values situated nearest to the particular grid-point, effectively resulting in nearest neighbour interpolation. In regions with a low density of stations, the long-range influence of a few individual values may then become too large. Therefore, as a compromise, at each grid-point, half-width h_a is defined as a linear function of the distance to the nearest station, $h_a(\mathbf{x}) = a_1 r_{\min}(\mathbf{x}) + a_2$, where $r_{\min}(\mathbf{x}) = \min |\mathbf{x} - \mathbf{x}_i|$.

3) Weighting function depending only on the absolute difference in DTC/DTO, with $a_0 = 0$ and $c_0 = \log(2)/h_c$. Since gradients in surface wind speed and air temperature at mean sea level can be expected to be largest near the coast, half-width is defined as a linear function of DTC/DTO, $h_c(\mathbf{x}) = c_1 D(\mathbf{x}) + c_2$.

4) Mixed weighting function, depending on horizontal distance and absolute difference in DTC/DTO, with $a_0(\mathbf{x}) = \log(2)/(a_1 r_{\min}(\mathbf{x}) + a_2)$, and $c_0(\mathbf{x}) = \log(2)/(c_1 D(\mathbf{x}) + c_2)$.

Determining the best interpolation technique is complicated by the fact that different measures of overall errors (such as mean errors and mean absolute errors) are minimised by different interpolation techniques and different sets of parameter values. The relative magnitude of errors of different interpolation techniques may also be different in different regions or in different months. For the purpose of kinetic and thermal energy conservation, the primary criterion here is the minimisation of mean errors, or biases. For interpolation techniques with similar overall biases, that method is chosen with the best balance between errors at coastal and inland regions, as well as between errors at low- and high-elevation sites. If further distinction is necessary, the emphasis is on the winter months, since then wind speeds are higher, and spatial variability is increased.

For a given interpolation technique, overall measures of errors depend on the set of available test stations. Adding or removing data points generally changes the results, especially if the relative number of coastal and inland stations changes, or the relative number of low- and high-elevation sites. The magnitude of these changes is estimated here by calculating biases and mean absolute errors (MAEs) repeatedly with different individual stations, or sets of stations, removed from the analysis. The standard deviations of these sets of errors are then used as uncertainty intervals for errors.

For surface wind speed, the best results are obtained with an interpolation technique through horizontal averaging, using a mixed weighting function, with $a_1 = 5.0$, $a_2 = 16.2$, $c_1 = 0.1$, and $c_2 = -0.1$, and the shortest horizontal distance to the open ocean, rather than to the coast. For types 2) and 3) of the weighting function, a combination of parameters can be found which provides better results than for linear radial basis functions. The largest mean absolute errors and regional biases result from a constant weighting function.

By contrast, for surface air temperature, the best results are obtained with horizontal interpolation using linear radial basis functions. Of the interpolation techniques using horizontal averaging, a mixed weighting function using DTO rather than DTC provided the best results.

For smooth fields with a high degree of spatial cross-correlation, such as surface air temperature, interpolation techniques preserving measured values are advantageous as far as the minimisation of biases and MAEs is concerned (see also the discussion in Gylfadóttir (2003) and Björnsson et al. (2007) about the use of best linear estimators, as in kriging). However, for fields with a high degree of spatial variability and local turbulent fluctuations, such as surface wind speed, interpolation through horizontal averaging provides overall better results. For surface wind speed, the influence of land–sea differences is significant and systematic enough, once the dominant effects of terrain elevation are removed, to improve the accuracy of horizontal interpolation, if DTO (and to a lesser extent DTC) is taken into account. Spatial coherence of wind speed is therefore determined by geographical similarity with respect to the distance from the coast or open ocean, in addition to horizontal proximity. For surface air temperature, projected to mean sea level, horizontal proximity is the most important predictor.

The local errors associated with the wind speed and temperature models, using the most accurate interpolation techniques, are shown in Figure 6. There are no regionally consistent patterns of positive or negative errors, either along the coast, or in the interior, for either of the two variables.

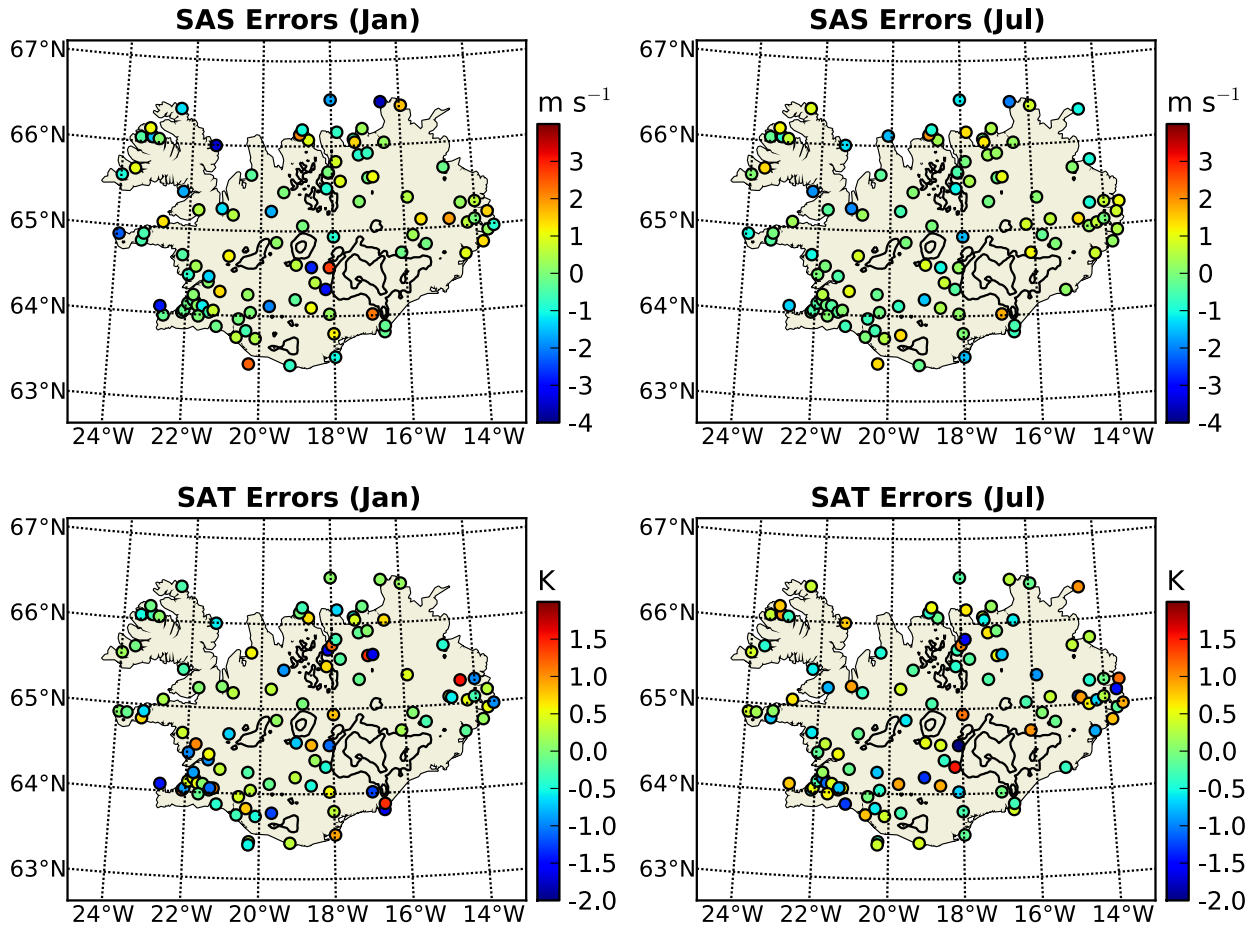


Figure 6. Errors associated with the one-parameter terrain models: differences are calculated between interpolated and actual surface wind speeds and air temperatures. Terrain elevation contour lines are drawn at 1000 and 1500 mASL.

The accuracy of the wind speed terrain model is primarily between $\pm 1.5 \text{ m s}^{-1}$, or between $\pm 30\%$ of the locally measured standard deviation. However, near steep terrain, or at exposed sites, deviations can be as large as $\pm 4 \text{ m s}^{-1}$, or about equal to the local standard deviation. Mean errors are small throughout the year, with 0.02 m s^{-1} in January, and 0.04 m s^{-1} in July. The uncertainty in overall bias is 0.012 m s^{-1} in January, and 0.008 m s^{-1} in July, if only one station at a time is removed from the different error analyses. Uncertainty increases to 0.020 m s^{-1} in January, and to 0.014 m s^{-1} in July, if all possible combinations of three different stations are removed from the error analyses. The MAE is 0.90 m s^{-1} in January, and 0.67 m s^{-1} in July. Uncertainties associated with these MAEs, resulting from the omission of three stations at a time, are 0.014 m s^{-1} in January, and 0.009 m s^{-1} in July. Overall, $\pm 1 \text{ m s}^{-1}$ can be taken as a realistic confidence interval for interpolated surface wind speeds. In percent of the local standard deviation, the MAE is 21% in January, and 26% in July. These errors are within the range of errors associated with the prediction of average wind speeds using the Wind Atlas Method (WASP) over complex terrain (Troen and Petersen, 1989; Petersen et al., 1997).

For surface air temperature, the differences between interpolated and measured values vary between $\pm 2 \text{ K}$, or between $\pm 30\%$ of the locally measured standard deviation. The extreme errors

are therefore in a similar range as those found by Björnsson et al. (2007). As for surface wind speed, mean errors are small throughout the year, with -0.02 in January, and 0.02 in July, and uncertainties associated with the omission of three stations at a time of 0.010 K in January and July. The MAE is 0.52 K in January, and 0.56 K in July, with uncertainties associated with the omission of three stations at a time of 0.007 K in January, and 0.006 K in July. In percent of the local standard deviation, the MAE is 18% in January, and 34% in July. For comparison, the biases of the eight-parameter model developed by Björnsson et al. (2007) are 0.05 K in January, and -0.04 K in July, with MAEs of 0.43 K in January, and 0.38 K in July. As mentioned above, as a matter of practical reality, improvements in mean errors result in increased mean absolute errors, and *vice versa*. However, for both models, biases and MAEs are within the range of radiative errors, associated with surface air measurements in standard enclosures (Nakamura and Mahrt, 2005).

5 Reference Values at Mean Sea Level

The seasonal cycle of vertical terrain gradients of surface wind speed, and the terrain lapse rates (the negative of terrain gradients) of air temperature are shown in Figure 7. Also shown are the corresponding atmospheric vertical gradients and lapse rates within the lowest 100 mAGL, derived from radiosonde data. These latter vertical gradients are first order finite differences between the values at 100 mAGL and the lowest data points. In the following section, they will be used to project surface variables to 100 mAGL. For wind speed, the seasonal cycles of vertical terrain gradient and atmospheric gradient are similar, with positive values throughout the year, and the largest values in winter, as the overlying flow intensifies. However, the low-level atmospheric gradient is about an order of magnitude larger. The terrain lapse rate of surface air temperature is positive throughout the year, with a similar annual average as the low-level atmospheric lapse rate at Keflavik, but following an opposite seasonal cycle. In summer, the elevated terrain in the interior of the island heats more strongly than low-lying coastal terrain, while even the low-lying terrain heats more strongly than the overlying atmosphere. As a result, the terrain lapse rate decreases in summer, whereas the low-level atmospheric lapse rate increases.

Measured and projected monthly averages of surface wind speed are shown in Figure 8. Since generally terrain elevation increases towards the interior of the island, the largest differences between actual and projected values are found there. Despite increased distances from the coast, due to the significant rise in elevation, and the low surface roughness of the terrain, surface wind speeds generally increase towards the centre of the island. However, as expected over flat terrain, after elevation effects are accounted for, surface wind speed tends to decrease away from the coast. On a regional basis, throughout the year, the lowest wind speeds at mean sea level exist in the northeastern interior part of the island. In coastal regions, the lowest wind speeds are found at the sheltered measurement sites in the Westfjords.

Measured and projected monthly averages of surface air temperature are shown in Figure 9. In winter, after elevation effects are accounted for, the differences between coastal and interior temperatures are significantly reduced, with interior temperatures only slightly colder than those along the coast, especially over the southern half of the island. In summer, the projected temperatures are fairly homogeneous throughout most of the island, with about 3 K lower temperatures along the eastern and northern coast.

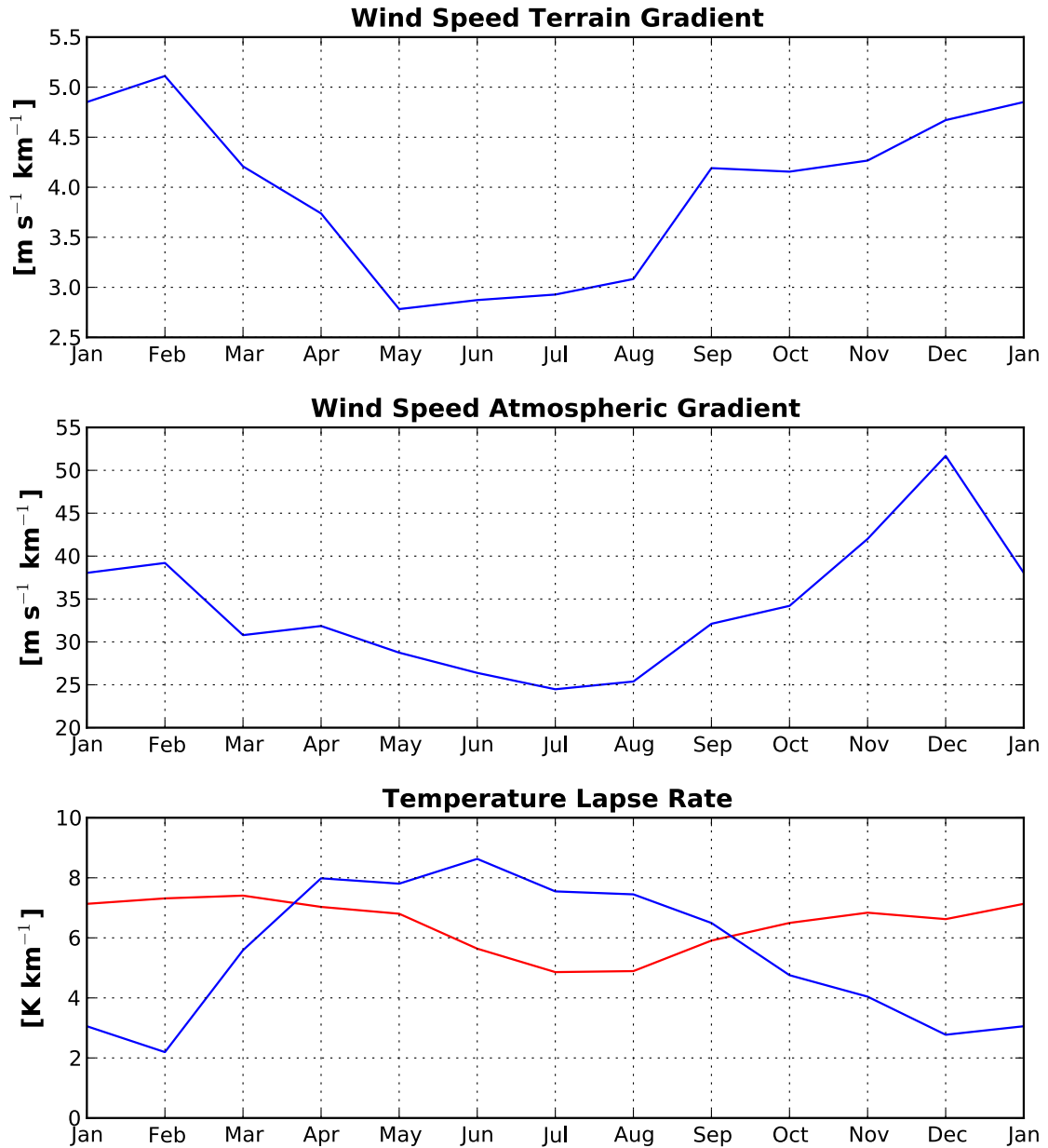


Figure 7. Monthly vertical gradients of wind speed over elevated terrain (top panel), and within the lowest 100 mAGL above Keflavík Airport (middle panel). Bottom panel: monthly temperature lapse rates over elevated terrain (red line), and within the lowest 100 mAGL above Keflavík Airport (blue line).

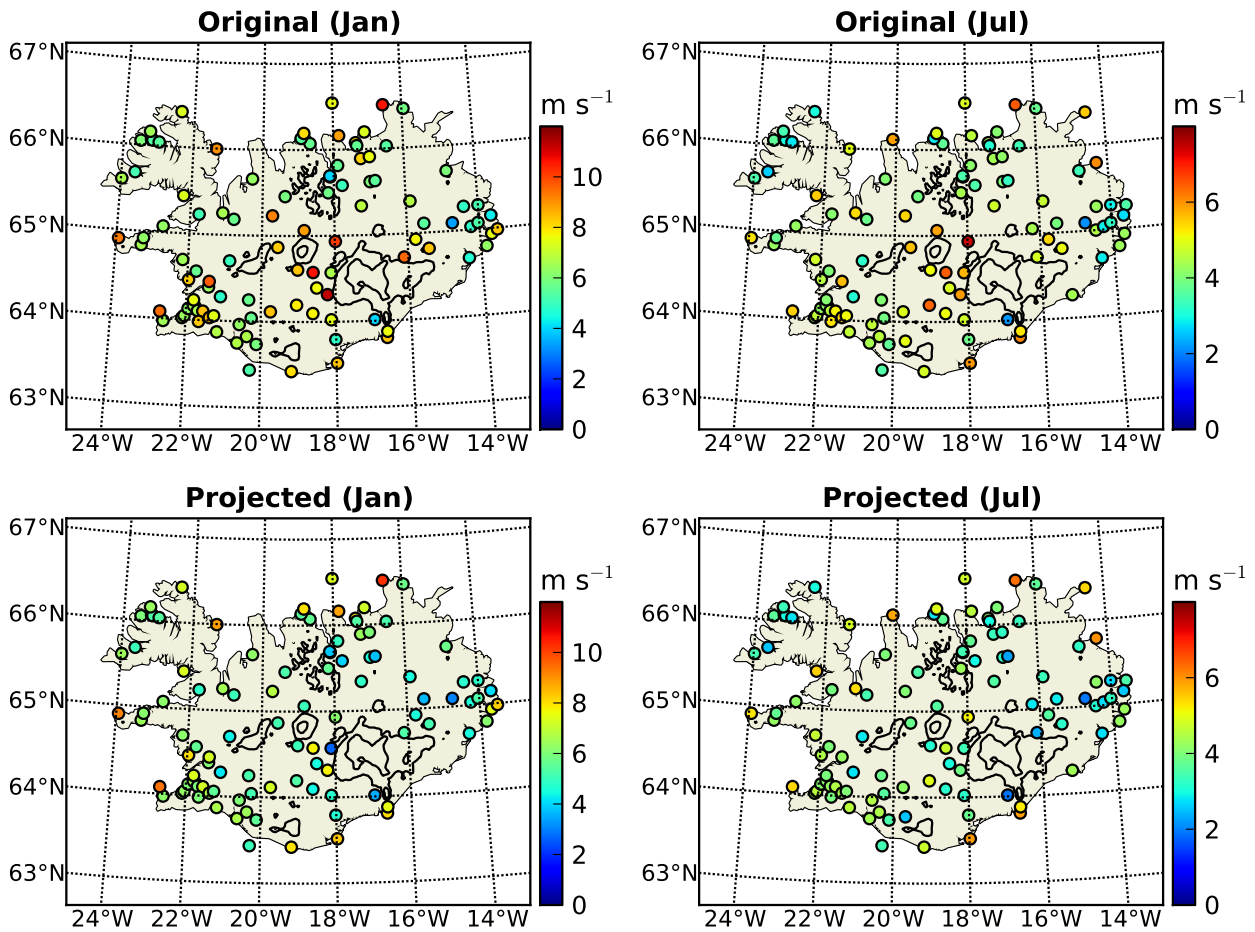


Figure 8. Monthly surface wind speeds at station locations: originally measured values (top panels), and projected to mean sea level based on the one-parameter terrain model (bottom panels).

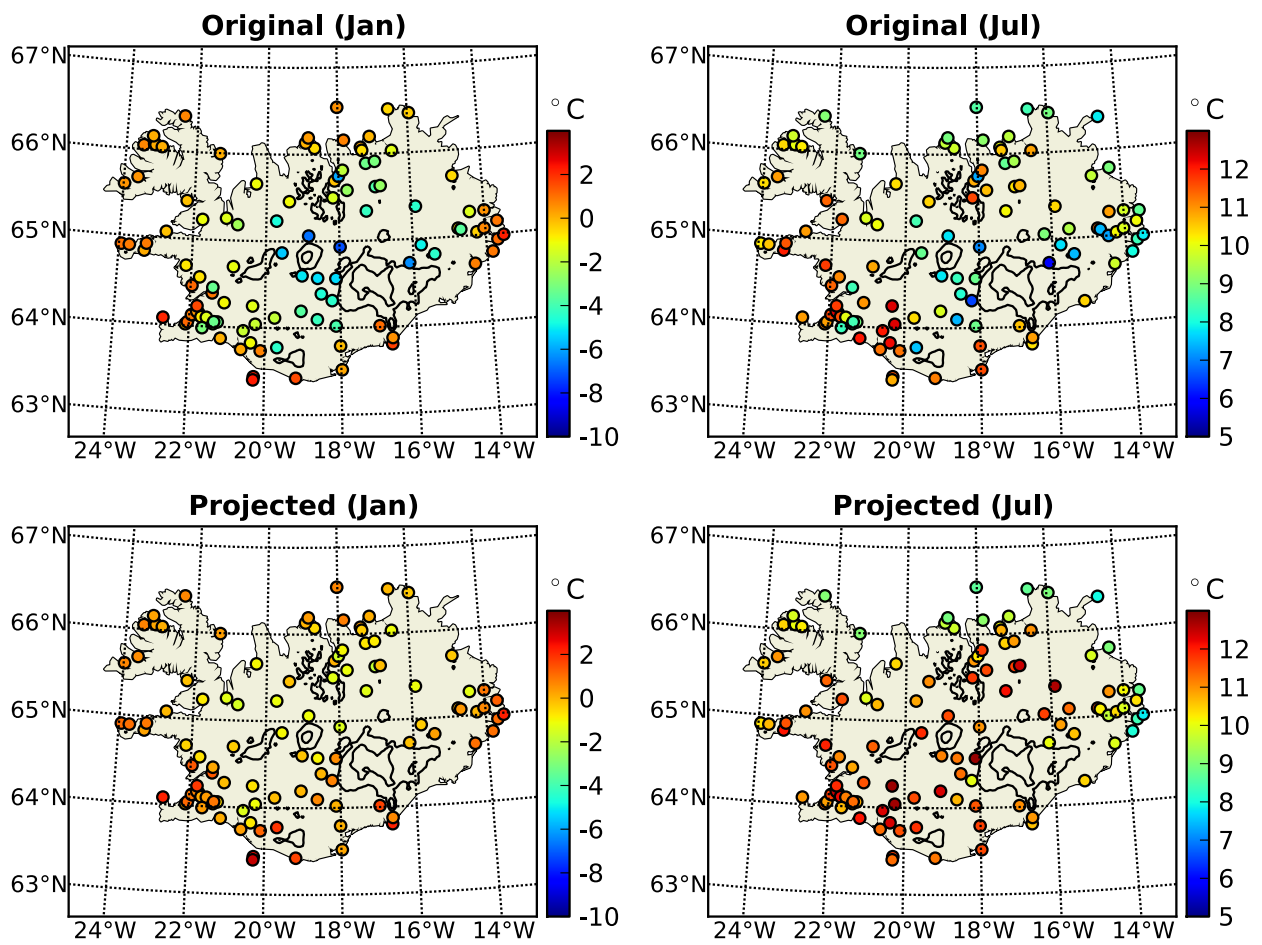


Figure 9. Monthly surface air temperatures at station locations: originally measured values (top panels), and projected to mean sea level based on the one-parameter terrain model (bottom panels).

6 Gridded Fields

Given a specific orography, the interpolated reference fields at mean sea level can be projected back onto elevated terrain. The orography used here is that of the WRF model. For surface variables, the appropriate sensor height is added to the terrain elevation, i.e., 10 m for wind speed, and 2 m for air temperature. Additionally, projections are calculated up to 100 mAGL, which is often taken as reference height for wind energy assessments. For this projection, the low-level atmospheric vertical gradients shown in Figure 7 are used.

As seen in Figure 3, monthly averaged wind speed based on the Keflavík radiosonde data increases rapidly within the lowest 200 mASL of the atmosphere, remaining essentially constant above 400 mASL. Due to that, it is realistic to assume, that the low-level atmospheric vertical gradients of wind speed above the low-lying upper-air station are larger than above higher elevations. In fact, it is well known from field studies, wind tunnel experiments, and numerical simulations, that over mountain tops and ridges, under neutral and stable conditions, with shallow and steep slopes, low-level speed maxima tend to form within the lowest few tens of metres above the ground, creating negative vertical wind speed gradients between the surface and 100 mAGL (e.g., Takahashia et al., 2002; Ross et al., 2004; Takahashia et al., 2005; Corbett et al., 2008). When projecting wind speeds to above the 10 mAGL surface layer, the large atmospheric vertical gradients are therefore only applied in full, if the resulting wind speed projected to 100 mAGL does not exceed that of the average Keflavík sounding at the same altitude above mean sea level. Otherwise, the value from the sounding profile is used. Over the highest terrain points of Vatnajökull and Hofsjökull, even the 10 mAGL wind speed according to the terrain model slightly exceeds the wind speed of the Keflavík sounding at the same altitude. The 100 mAGL speed chosen from the sounding is then somewhat lower than the 10 mAGL speed, forming low-level jets.

Gridded fields of wind speed at 10 and 100 mAGL for January and July are shown in Figure 10. The range of values at 10 mAGL is $5 - 14 \text{ m s}^{-1}$ in January, and $3 - 9 \text{ m s}^{-1}$ in July. By comparison, the range of local values projected to mean sea level is $2 - 10 \text{ m s}^{-1}$ in January, and $1 - 6 \text{ m s}^{-1}$ in July (see Figure 8). Purely horizontal differences in wind speed are therefore comparable to the overall spatial variability, including effects of terrain elevation. With an increase (decrease) in the lowest (highest) wind speeds at 100 mAGL, compared with those at 10 mAGL, the spatial range is reduced by more than one half to $9 - 13 \text{ m s}^{-1}$ in January, and $6 - 8 \text{ m s}^{-1}$ in July.

The interpolated monthly fields of horizontal wind at mean seal level for day- and night-time conditions in January and July are shown in Figure 11.² For the 3-hourly time-series, day is defined as 09:00 – 18:00 UTC, or local time, and night is defined as 21:00 – 06:00 UTC. In winter, prevailing downslope and offshore surface wind occurs across Iceland, with negligible differences between day and night. In summer, significant differences exist, both in speed and direction, between day- and night-time surface wind conditions. During the night, there are only small changes in the directional wind field, compared with winter, over the southwest part of the island. In the northeast, weak onshore winds exist even at night. Across the island, onshore and upslope winds develop fully during the day. Based on local station data, the seasonal change in surface wind conditions was discussed in Nawri et al. (2012c). For the month of June, the increase

²The stereographic projection of wind vectors employed for these figures is described in Nawri et al. (2012c).

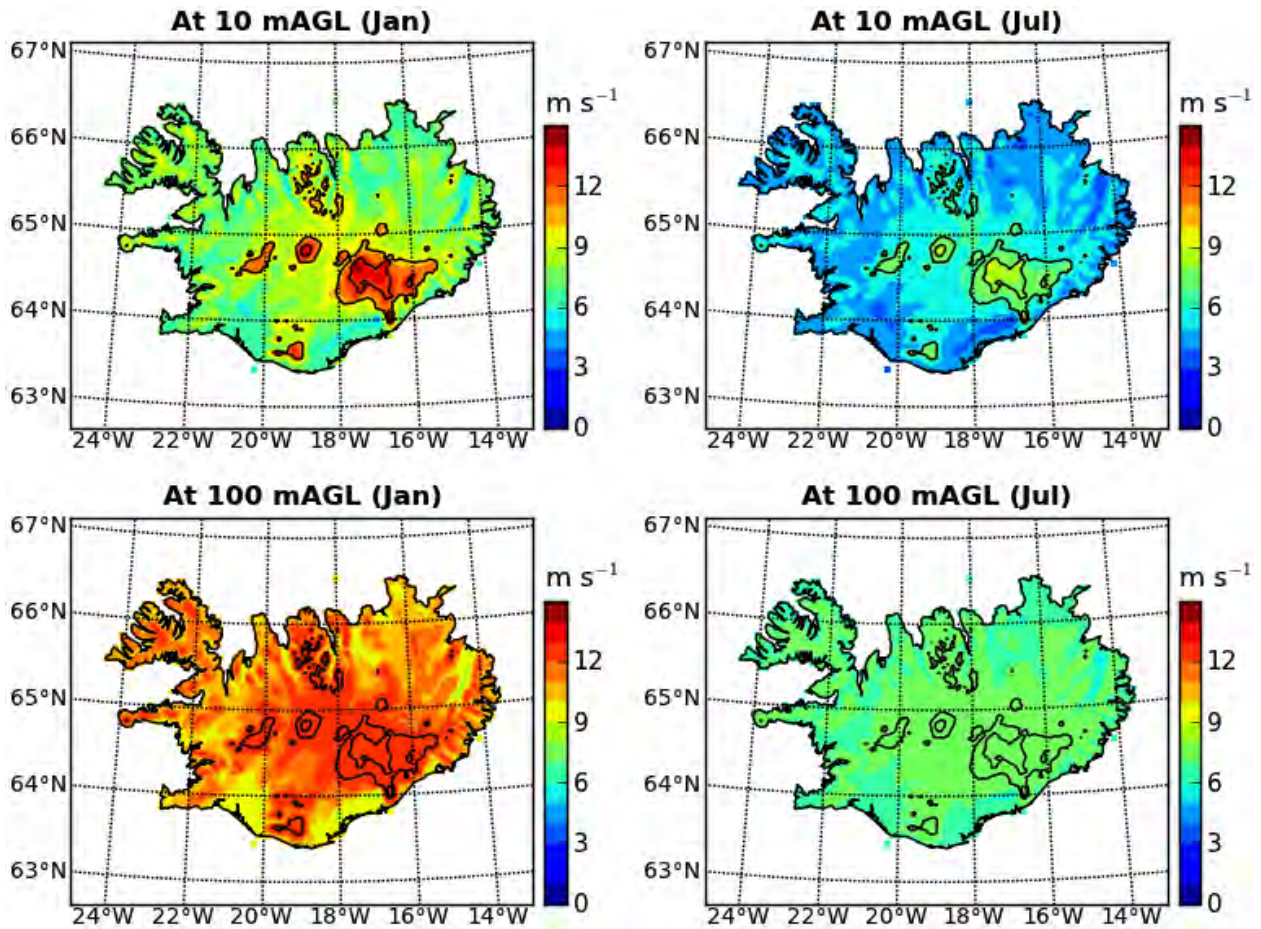


Figure 10. Gridded wind speed based on the one-parameter terrain model at 10 and 100 mAGL.

in surface wind speed during the day, and the prevailing daytime onshore and upslope winds have previously been documented by Jónsson (2002).

This contrast between winter- and summertime wind conditions, as well as between day- and nighttime conditions in summer, strongly suggests a dominance of thermal forcing for the determination of the prevailing directions of low-level winds, relative to other forcing mechanisms. This is supported by the significant increase in average monthly sunshine hours from January to July, with 26.9 hours in January, and 171.3 hours in July at Reykjavík in the southeast, and 7.0 hours in January, and 158.0 hours in July at Akureyri in the north (sunshine data is available online from the Icelandic Meteorological Office at <http://www.vedur.is/vedur/vedurfar/medaltalstoflur/>; the averaging period for monthly totals is 1961 – 90). The main exceptions to the seasonal change in surface wind directions exist over outlying parts of the island, such as the Westfjords and Snæfellsnes, where the land areas are insufficient to create strong thermal contrasts to the surrounding ocean. In these regions, winds are affected by the large-scale circulation, rather than by local thermal effects (Nawri et al., 2012c).

Unlike the atmospheric vertical wind speed profiles, average temperature gradients are constant throughout the boundary-layer (see Figure 5). Therefore, for the projection of temperatures from

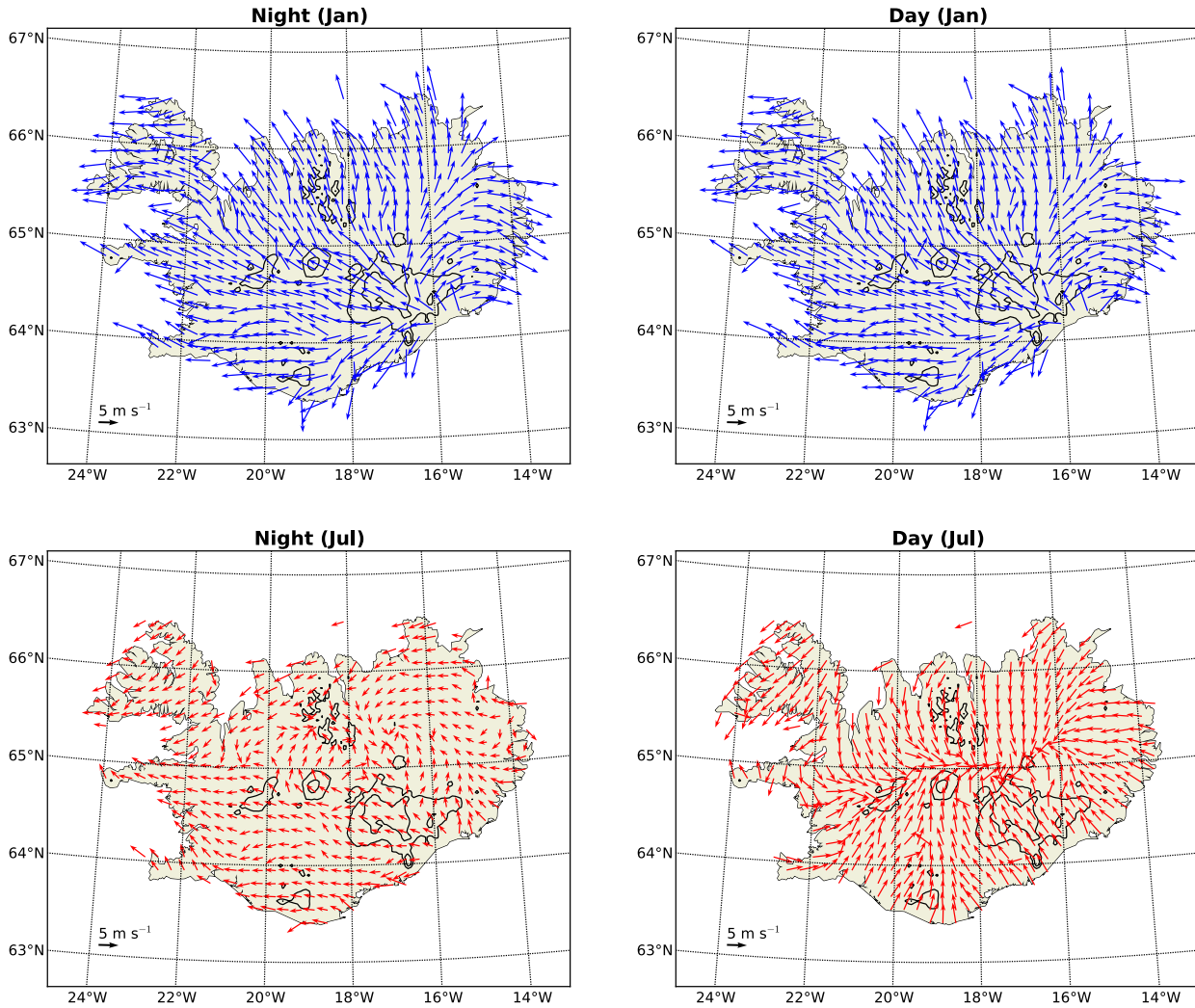


Figure 11. Gridded horizontal wind vectors at mean sea level based on the one-parameter terrain model, for night- and day-time conditions in January and July.

2 to 100 mAGL, the low-level atmospheric lapse rates, shown in Figure 7, are applied uniformly at all elevations, whether along the coast or in the interior of the island.

Gridded fields of air temperature at 2 and 100 mAGL for January and July are shown in Figure 12. The range of values at 2 and 100 mAGL is $-12 - 2^{\circ}\text{C}$ in January, and $2 - 12^{\circ}\text{C}$ in July, compared with a range of local values projected to mean sea level of $-2 - 4^{\circ}\text{C}$ in January, and $8 - 14^{\circ}\text{C}$ in July (see Figure 9). Throughout the year, purely horizontal differences in air temperature are therefore about half the differences associated with the overall spatial variability, and low-level air temperatures are significantly determined by terrain elevation. Despite the non-overlapping data periods, and aside from the different spatial resolutions, the results shown in Figure 12 are consistent with those obtained by Björnsson et al. (2007), using different parameterisation and interpolation techniques. Generally, the differences between the terrain model presented here and the previous model are of the same magnitude as the inherent uncertainties in either of the models (refer again to Section 4). In comparison with the constant lapse-rate model derived by Crochet

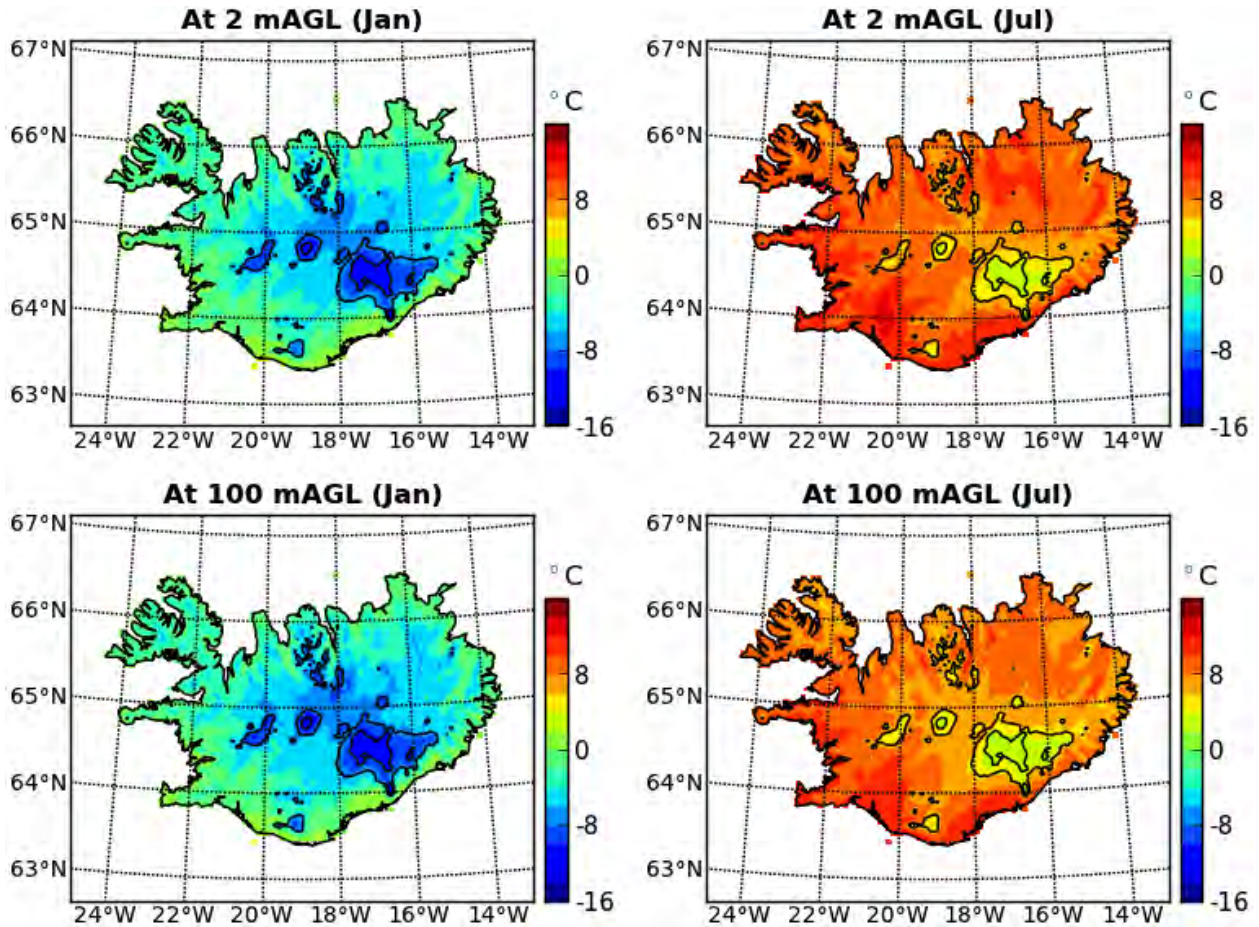


Figure 12. Gridded air temperature based on the one-parameter terrain model at 2 and 100 mAGL.

and Jóhannesson (2011), there are some systematic differences, which are related to the seasonal cycle of the lapse-rate of the terrain model developed here. The variable lapse-rate used here (see again Figure 7) is between $0.5 - 1.0 \text{ K km}^{-1}$ higher than the constant value (6.5 K km^{-1}) in winter, and between $1 - 2 \text{ K km}^{-1}$ lower in summer. This leads to an increased seasonal cycle at high elevations compared with the constant lapse-rate model, with lower values in winter, and higher values in summer. At lower elevations, differences are negligible, and primarily related to differences in the terrain used.

7 Effects of the Large-Scale Atmospheric Circulation

As discussed in previous sections, and in more detail in Nawri et al. (2012c), the surface wind conditions over Iceland are greatly influenced by local terrain effects, as well as by land–sea differences along the coast. In this section, the effects of the larger-scale atmospheric circulation on surface wind conditions over Iceland will be analysed.

As a representation of the prevailing large-scale flow over Iceland, the geostrophic wind is calculated from ECMWF operational analyses of the geopotential height at 850 hPa. Throughout the year, this level oscillates between about 900 and 1650 mASL over the island. It is therefore consistently above the highest station locations, but below the highest terrain tops. As shown in Figure 3, on a monthly average basis, wind speed in the coastal boundary-layer above Keflavik is constant with height from about 400 mASL upwards. This level can therefore be taken as the typical height at the top of the boundary-layer at low elevations. With higher terrain elevation, the top of the boundary-layer is necessarily raised. Therefore, as a compromise for the whole island, the 850 hPa level is taken here to represent the lowest level of the free atmosphere.

The regional geostrophic wind speed is calculated from the average magnitude of the geopotential height gradient over the land area of Iceland, according to the land-sea mask of the operational analyses, whereby grid-point values are weighted by the cosine of latitude, to take into account the area represented by each grid-point. For each month, the geostrophic wind speeds at 850 hPa are then separated into three classes of wind speed:

- Weak geostrophic winds with speeds less than or equal to the monthly 30th percentile (varying between $3.7\text{--}8.3\text{ m s}^{-1}$),
- Intermediate geostrophic winds with speeds greater than the 30th, and less than or equal to the 65th monthly percentile (varying between $7.2\text{--}14.9\text{ m s}^{-1}$),
- Strong geostrophic winds with speeds greater than the 65th monthly percentile.

As shown in Figure 13, under weak and intermediate large-scale pressure gradients, the monthly correlation between the geostrophic wind speed and measured surface wind speed at individual locations is generally poor. At some locations, correlation between surface and geostrophic wind speed improves with increasing strength of the overlying circulation, especially in winter. At most locations, however, the temporal correlation with the large-scale flow remains insignificant. The two regions with consistently low correlations are the Westfjords and the central part of the eastern region. Correlations there are not improved by calculating the geostrophic wind at 850 hPa exclusively from the nearest grid-point, rather than from all land grid-points (not shown). Overall, despite some high-correlation sites, fluctuations around monthly averages of surface wind speeds over Iceland are poorly correlated with fluctuations of the larger-scale flow, as represented by ECMWF operational analyses.³

Local correlations of the complete time-series, not just for individual months, and taking into account all geostrophic wind speeds, are shown in Figure 14. Prior to calculating correlations, time-series were smoothed by the application of temporal running-means over periods from 1 to 30 days. Correlations at high-correlation sites are further increased for 1-day running means, compared with the original time-series. Generally, for increasing smoothing periods greater than one day, correlations increase at low-correlation sites, and decrease at high-correlation sites. Average correlations increase from 0.187 for the original time-series to 0.379 for 15-day running means, but decrease again to 0.351 for 30-day running means. Therefore, the strongest and most consistent response of surface wind speeds to fluctuations in the geostrophic wind occurs on time-scales associated with cyclonic activity.

³The correlations discussed here are calculated for 3-hourly time-series, requiring operational analyses to be linearly interpolated in time. However, differences to correlations calculated for 6-hourly time-series are negligible.

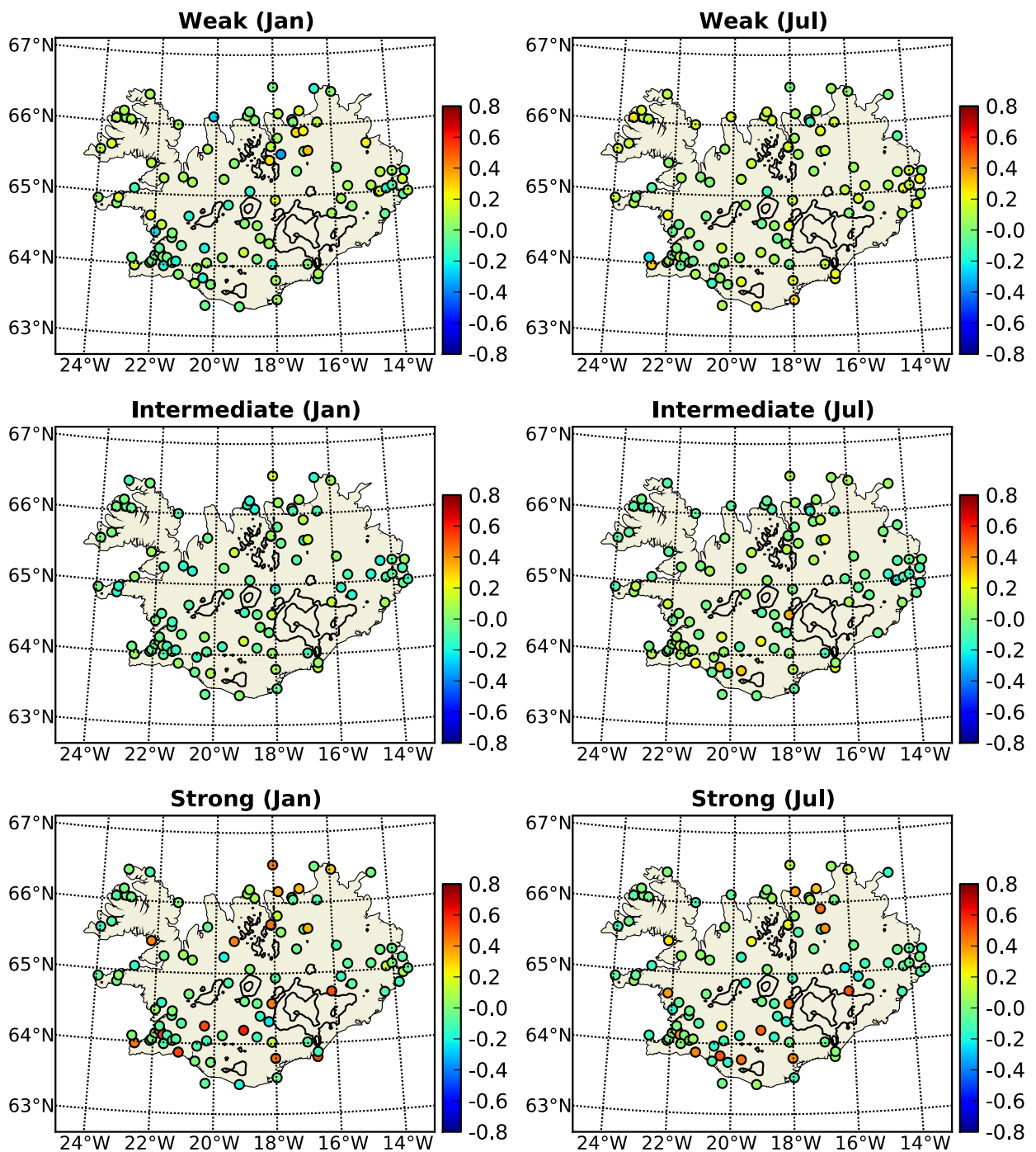


Figure 13. Correlation between surface air speed at station locations and geostrophic wind speed at 850 hPa for different intensity of the geostrophic wind speed (see Section 7).

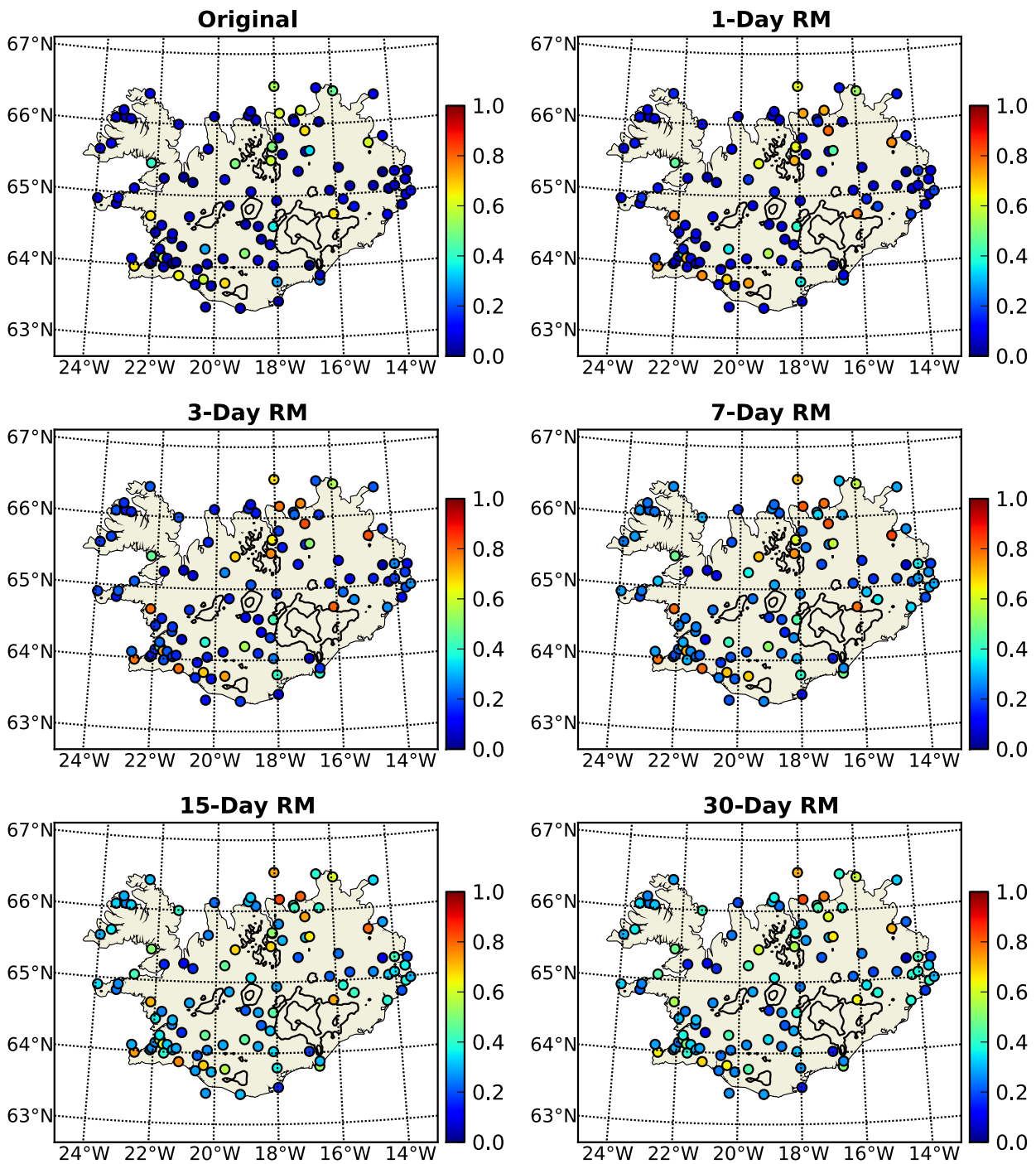


Figure 14. Correlation between measured surface wind speed and geostrophic wind speed at 850 hPa, for the original 3-hourly time-series, as well as for time-series which are smoothed by temporal running means (RM) over different time-periods.

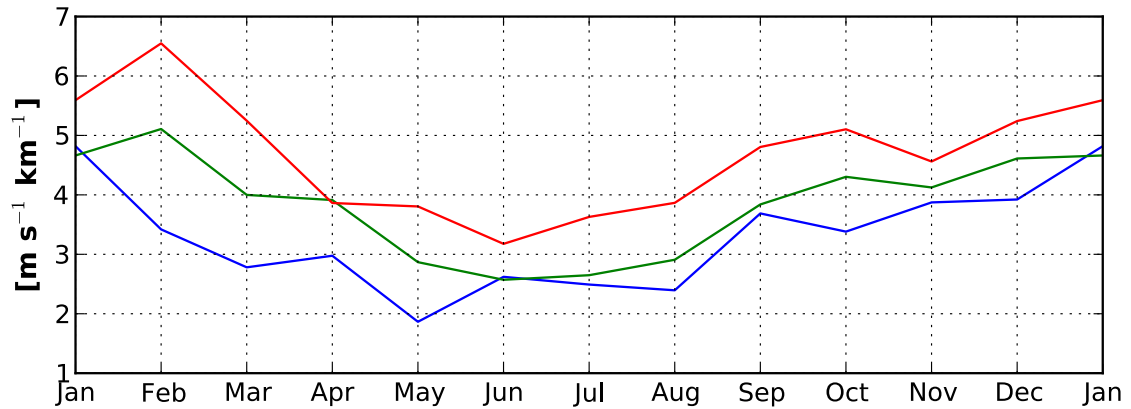


Figure 15. Vertical terrain gradients of surface wind speed for weak (blue line), intermediate (green line), and strong (red line) geostrophic wind speeds at 850 hPa (see Section 7).

The vertical terrain gradients of monthly mean surface wind speed are systematically affected by an increasing strength of the large-scale atmospheric circulation, as represented by operational analyses (see Figure 15). For each intensity class of the geostrophic wind speed, terrain gradients follow a qualitatively similar seasonal cycle to that of the average geostrophic wind speed in the given intensity class (not shown), with the highest values in winter, and the lowest values in summer. Additionally, terrain gradients of surface wind speed in each month increase with the intensity of the overlying flow. If upper-level winds are accurately portrayed by operational analyses, throughout the year, low-level speed shear is significantly increased under conditions of strong overlying flow.

Surface wind speeds based on the terrain models corresponding to these vertical gradients are shown in Figure 16. Despite significant sheltering and low temporal correlations at many locations, on a monthly basis, surface wind speed generally increases with increasing strength of the overlying flow, as represented by the ECMWF geostrophic wind at 850 hPa, especially at intermediate and high elevations.

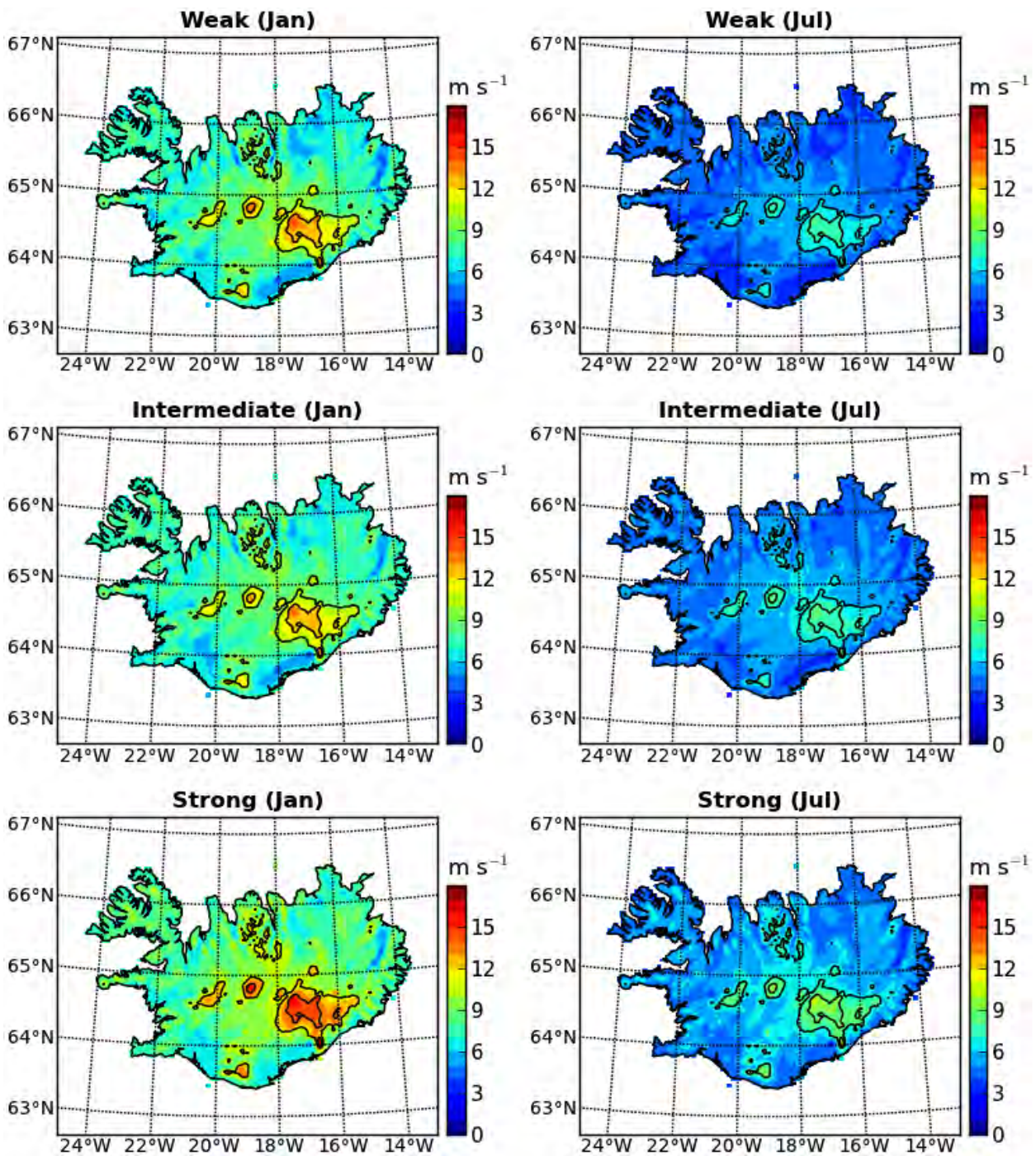


Figure 16. Gridded surface wind speed based on the one-parameter terrain model for different geostrophic wind speeds (see Section 7).

8 Summary

In this study, one-parameter terrain models for surface wind speed and air temperature were developed based on station data. These models enable the study of regional differences by reducing the effects of different terrain elevations, as well as allowing horizontal interpolation between measurement sites.

Despite increased distances from the coast, due to the significant rise in elevation, and the low surface roughness of the terrain, surface wind speeds generally increase towards the centre of the island. However, as expected over flat terrain, after elevation effects are accounted for, surface wind speed tends to decrease away from the coast. On a regional basis, throughout the year, the lowest wind speeds at mean sea level exist in the northeastern interior part of the island. In coastal regions, the lowest wind speeds are found at the sheltered measurement sites in the Westfjords.

In winter, prevailing downslope and offshore surface wind occurs across Iceland, with negligible differences between day and night. In summer, significant differences exist, both in speed and direction, between day- and night-time surface wind conditions. During the night, there are only small changes in the directional wind field, compared with winter, over the southwest part of the island. In the northeast, weak onshore winds exist even at night. Across the island, onshore and upslope winds develop fully during the day. The main exceptions to the seasonal change in surface wind directions exist over outlying parts of the island, such as the Westfjords and Snæfellsnes, where the land areas are insufficient to create strong thermal contrasts to the surrounding ocean. In these regions, winds are affected by the large-scale circulation, rather than by local thermal effects.

Under weak and intermediate large-scale pressure gradients, the monthly correlation between the geostrophic wind speed and measured surface wind speed at individual locations is generally poor. At some locations, correlation between surface and geostrophic wind speed improves with increasing strength of the overlying circulation, especially in winter. At most locations, however, the temporal correlation with the large-scale flow remains insignificant. The two regions with consistently low correlations are the Westfjords and the central part of the eastern region. Correlations at high-correlation sites are further increased for 1-day running means, compared with the original time-series. Generally, for increasing smoothing periods greater than one day, correlations increase at low-correlation sites, and decrease at high-correlation sites. Average correlations are highest for 15-day running means. Therefore, the strongest and most consistent response of surface wind speeds to fluctuations in the geostrophic wind occurs on time-scales associated with cyclonic activity.

Despite significant sheltering and low temporal correlations at many locations, on a monthly basis, surface wind speed generally increases with increasing strength of the geostrophic wind at 850 hPa, especially at intermediate and high elevations. Therefore, throughout the year, low-level speed shear is significantly increased under conditions of strong overlying flow.

In winter, after elevation effects are accounted for, the differences between coastal and interior temperatures are significantly reduced, with interior temperatures only slightly colder than those along the coast, especially over the southern half of Iceland. In summer, the projected temperatures are fairly homogeneous throughout most of the island, with about 3°C lower temperatures along the eastern and northern coast.

References

- Björnsson, H., Jónsson, T., Gylfadóttir, S. S., and Ólason, E. Ó. (2007). Mapping the annual cycle of temperature in Iceland. *Meteorol. Z.*, 16(1):45–56.
- Corbett, J.-F., Ott, S., and Landberg, L. (2008). A mixed spectral-integration model for neutral mean wind flow over hills. *Boundary-Layer Meteorol.*, 128:229–254.
- Crochet, P. and Jóhannesson, T. (2011). A data set of gridded daily temperature in Iceland, 1949–2010. *Jökull*, 61:1–18.
- Gylfadóttir, S. S. (2003). Spatial interpolation of Icelandic monthly mean temperature data. Report VÍ-ÚR06 03006, Icelandic Meteorological Office, Reykjavik, Iceland.
- Jónsson, T. (2002). Frumstæð athugun á dægursveiflu vindhraða og vindáttar í júnímánuði. Report VÍ-ÚR18, Icelandic Meteorological Office, Reykjavik, Iceland.
- Nakamura, R. and Mahrt, L. (2005). Air temperature measurement errors in naturally ventilated radiation shields. *J. Atmos. Oceanic Technol.*, 22:1046–1058.
- Nawri, N., Björnsson, H., Jónasson, K., and Petersen, G. N. (2012a). Evaluation of WRF mesoscale model simulations of surface wind over Iceland. Report VÍ 2012-010, Icelandic Meteorological Office, Reykjavik, Iceland.
- Nawri, N., Björnsson, H., Jónasson, K., and Petersen, G. N. (2012b). Statistical correction of WRF mesoscale model simulations of surface wind over Iceland based on station data. Report VÍ 2012-011, Icelandic Meteorological Office, Reykjavik, Iceland.
- Nawri, N., Björnsson, H., Jónasson, K., and Petersen, G. N. (2012c). Surface wind and air temperature over Iceland based on station records and ECMWF Operational Analyses. Report VÍ 2012-008, Icelandic Meteorological Office, Reykjavik, Iceland.
- Petersen, E. L., Mortensen, N. G., Landberg, L., Højstrup, J., and Frank, H. P. (1997). Wind power meteorology. Report Risø-I-1206(EN), Risø National Laboratory, Roskilde, Denmark.
- Rögnvaldsson, Ó., Ágústsson, H., Einarsson, E. M., Ólafsson, H., Björnsson, H., and Sveinsson, Ó. G. B. (2007). Stöðuskýrsla vegna fyrsta árs RÁV verkefnisins. Technical report, Reiknistofa í veðurfræði, Reykjavik, Iceland.
- Rögnvaldsson, Ó., Ágústsson, H., and Ólafsson, H. (2011). Aflræn niðurkvörðun veðurs innan LOKS verkefnisins. Technical report, Reiknistofa í veðurfræði, Reykjavik, Iceland.
- Ross, A. N., Arnold, S., Vosper, S. B., Mobbs, S. D., Dixon, N., and Robins, A. G. (2004). A comparison of wind-tunnel experiments and numerical simulations of neutral and stratified flow over a hill. *Boundary-Layer Meteorol.*, 113:427–459.
- Skamarock, W. C., Klemp, J. B., Dudhia, J., Gill, D. O., Barker, D. M., Duda, M. G., Huang, X.-Y., Wang, W., and Powers, J. G. (2008). A description of the Advanced Research WRF Version 3. NCAR Technical Note NCAR/TN-475+STR, National Center for Atmospheric Research, Boulder, Colorado, USA.

- Takahashia, T., Katoa, S., Murakamib, S., Ookaa, R., Yassinc, M. F., and Kono, R. (2005). Wind tunnel tests of effects of atmospheric stability on turbulent flow over a three-dimensional hill. *J. Wind Eng. Ind. Aerodyn.*, 93:155–169.
- Takahashia, T., Ohtsua, T., Yassina, M., Katoa, S., and Murakami, S. (2002). Turbulence characteristics of wind over a hill with a rough surface. *J. Wind Eng. Ind. Aerodyn.*, 90:1697–1706.
- Troen, I. and Petersen, E. L. (1989). *European Wind Atlas*. Risø National Laboratory, Roskilde, Denmark.
- WMO (2008). *Guide to Meteorological Instruments and Methods of Observation, WMO-No. 8, 7th Edition*. World Meteorological Organization, Geneva, Switzerland.